



Published in final edited form as:

ACS Macro Lett. 2013 August 20; 2(8): 710–714. doi:10.1021/mz400370f.

Water-soluble Semiconducting Nanoparticles for Imaging

Chinessa T. Adkins, Julia N. Dobish, Scott Brown, and Eva Harth*

Department of Chemistry, Vanderbilt University, 7619 Stevenson Center, Nashville, Tennessee, USA

Abstract

Water-soluble semiconducting nanoparticles are prepared from individually collapsed and crosslinked ABA triblock copolymers and are further modified to carry imaging units and allyl functionalities for postmodification. Ethylene oxide modified polyfluorene forms the center block (B) and is transformed into a telechelic macroinitiator. In a nitroxide mediated living free radical polymerization, polyacrylate blocks (A) are grown to give the ABA triblock copolymer. Low-temperature benzocyclobutene crosslinking groups are attached to collapse and site-isolate the center block (A). The nanoparticles were further modified by pegylation to enhance the solubility and by catechol groups to provide complexing sites for magnetic resonance imaging (MRI) reagents such as gadolinium. The reported materials are water-soluble and encompassing fluorescence and MRI to become biocompatible “organic quantum dots” with the possibility to interact actively with biological entities.

Keywords

Water soluble organic quantum dots; MRI imaging; biosensing; site isolation of fluorophores; intermolecular chain collapse

The combination of fluorescence microscopy with molecular imaging techniques are leading to a rapid proliferation of advanced fluorescence based techniques in chemistry and the life sciences.¹ These methods can be utilized for the imaging of biomolecular interactions within a single molecule and have the ability to further our understanding of various biochemical processes. The extension of fluorescence methods to living systems promises to provide an unprecedented understanding about cellular procedures through vital imaging techniques.^{2–4} However, two problems associated with fluorescence microscopy – cell autofluorescence in the visible spectrum and the requirement of long observation times – have created a need for new probes that emit in the near infrared (NIR) region (wavelength >700 nm). The application of these methods to living cells is further hindered by the current lack of dyes that are sufficiently bright and photostable to overcome the background fluorescence and scattering within the cell. The limited brightness of conventional dyes and cellular autofluorescence results in signal-to-background ratios that is too low for significant detection. The most photostable dyes such as Rhodamine 6G are subject to photobleaching and are insufficient for long term fluorescence tracking.⁵ In addition, fluorescence intermittency (“blinking”) of fluorescent dyes and quantum dots can further complicate imaging techniques.

Corresponding Author. eva.harth@vanderbilt.edu.

ASSOCIATED CONTENT

Supporting Information. Synthesis of polymers, nanoparticles as well as characterization methods are described. (<http://pubs.acs.org/page/jacsat/submission/authors.html>).

A number of different strategies for developing brighter fluorescent probes have been pursued. Fluorescent nanoparticles such as colloidal semiconductor quantum dots are under active development.⁶ However, these nanoparticles typically require an inorganic shell and a thick encapsulation layer to reach the required levels of stability and biocompatibility, resulting in large diameters which can significantly alter biological function and transport of the biomolecules. While there has been recent work to reduce the thickness of the biocompatibility and encapsulation layers,⁷ low emission rates, blinking, and a significant fraction of “dark” particles continue to pose potential difficulties for single particle measurements.⁸ Dye-loaded latex or silica beads also possess relatively large sizes and limited dye-loading concentration due to aggregation and self-quenching.⁹ These limitations of current luminescent particles provide motivation for the exploration of alternative approaches toward the design of more highly fluorescent nanoparticles. One promising strategy is the development of nanoparticles based on highly fluorescent π -conjugated polymers. There has been steady progress in the development of highly fluorescent π -conjugated polymers as the active material in polymer light-emitting devices.^{10,11} Also, conjugated polyelectrolytes have been demonstrated for application as highly sensitive biosensors.^{12,13}

The ability to tune properties of bulk materials has been extensively pursued by directed self-assembly of block copolymers, in both solution and in the solid state, to form well-defined phase separated structures or nanoobjects.¹⁴ Recent advances in synthetic polymer chemistry have enabled the preparation of a much wider variety of well-defined di- and multiblock copolymers¹⁵ and these systems demonstrate that the morphology and properties of polymeric materials can be dictated by composition, molar mass and architecture of the copolymer segments. Of these structural aspects, architecture is the most poorly studied, yet it has the potential to be an extremely powerful tool for controlling material properties.

Moreover, the introduction of MRI applications, add to the versatility of the resulting materials. MRI has become one of the most powerful techniques in early medical diagnostics. This methodology is characterized by its high resolution of soft tissues and by its evasion to radiation and is further enhanced by the use of contrast agents. Gd-DTPA (commercially known as Magnevist[®]) is the most commonly used MRI contrast agent that shortens the T_1 longitudinal relaxation time of protons of water and that increases the contrast of the image owing to the shortened relaxation time. However, this low molecular weight contrast agent has significant problems such as a short half-life in blood and lack of specificity to target organs and tissues for diagnosis. Macromolecular carriers have been examined for increases in relaxivity and specificity. Studied carriers include dendrimers,^{16–18} dextrans,^{19,20} polysaccharides,^{21,22} disulfide based biodegradable synthetic polymers,²³ PEG-grafted poly(L-lysine),²⁴ and conjugates of polymers and targeting moieties such as antibodies²⁵ and folates.²⁶ DTPA or other chelating units were conjugated to these polymeric carriers. None of these, however, have accomplished increases in both relaxivity and in specificity. As a result of these concerns, no macromolecular contrast agent has been approved for clinical use. Recently, star polymers have been increasingly investigated and have achieved high relaxivity values due to their unique architecture.^{27–29} However, the tendency to accumulate in organs such as the heart has limited the applicability to image other organs or tissues.²⁸ Alternatively, there are some attempts for the attainment of tumor specific MRI contrast agents, and these attempts utilize pH^{30,31} or enzymatic activity.³²

Herein, we explore the preparation of water soluble polymer nanoparticles from intramolecular chain collapse techniques and investigate their photophysical characteristics relevant for applications such as fluorescent and magnetic imaging in vivo and in vitro. These polymer systems show remarkable improvements in terms of their fluorescence

quantum yield as compared to previously reported systems. The extraordinary brightness of the chain collapsed nanoparticles and small particle diameters make them promising probes for demanding fluorescence applications. Several characteristics distinguish chain collapsed nanoparticles from the commonly used fluorophores including the ease for post-modification which allow the conjugation of chelating units for the incorporation of metals affording magnetic features.

Results and Discussion

The development of water soluble semiconducting nanoparticles required the use of an intramolecular chain collapse technique to afford a stable three-dimensional structure. This procedure necessitates the synthesis of an ABA block copolymer from a water soluble fluorene monomer serving as the B block with t-butyl acrylate and crosslinking units as the A block. For this reason, we chose to synthesize an ethylene oxide (EO) substituted dibromo fluorene through the use of commercially available 2,7-dibromofluorene and substituted EO units at the remote C₉ site. This allowed the preparation of a semiconducting telechelic macroinitiator from the EO fluorene monomer through a Yamamoto reaction utilizing Ni(COD)₂ as catalyst, producing a semiconducting telechelic macroinitiator.³³

The material was characterized through nuclear magnetic resonance (NMR) and gel permeation chromatography (GPC), which verified polymerization of the conjugated system from the apparent GPC MW of 13,000 Da with a polydispersity of 4.79, which is commensurate with typical Yamamoto conditions prior to purification.³⁴ Since SEC measurements of polyfluorenes (PS, calibration) typically display inaccurate values for M_w due to the rigid-rod or, better, semirigid-rod nature of the polymers, NMR measurements were employed which tend to display more accurate molecular weight measurements. NMR experiments on the resulting EO fluorene macroinitiator displayed absolute M_w values of 19,000 Da in relation to PS-calibrated standards (Table 1). This reflects the semirigid nature of the chains, a result of the distorted arrangement of the fluorene structural units.

Formation of the linear precursor required the introduction of t-butyl acrylate for solubility along with 5% low temperature crosslinker, 2-(1,2-dihydrocyclobutabenzene-1-yloxy)ethanamine,³⁵ (Scheme 1). Successful polymerization was verified by GPC which revealed an M_w of 67,000 Da with a PDI of 4.31 and the reduction of the PDI is attributed to the livingness of the controlled radical polymerization. Absolute molecular weight measurements via NMR presented an M_w of 96,000, signifying a 2:1:2 ratio of t-butyl acrylate to fluorene to t-butyl acrylate. Reaction of linear precursor, **4**, with trifluoroacetic acid (TFA) in dichloromethane was appropriate for the removal of t-butyl protecting groups which was confirmed through NMR spectroscopy. Complete elimination of the protecting groups from the acrylates was evident by the disappearance of protons in the 1.0 – 2.1 ppm region, as well as the alteration of solubility. Prior to deprotection, the linear precursor was only soluble in organic solvents such as dichloromethane and chloroform. However, after complete deprotection, the material was fully soluble in methanol. Characterization by UV-Vis and fluorescence spectroscopy revealed absorption and emission peaks at 370 nm and 438 nm, respectively and displayed a quantum efficiency of 2.8%.

Nanoparticle formation was induced through a controlled intramolecular chain collapse process which entails the dropping in of an ultra-dilute linear polymer precursor solution into a hot solvent solution to form particles in a defined size regime. As compared to other nanoparticle synthesis techniques, this particular method required temperatures as low as 150 °C³⁵ as opposed to the previously reported 250 °C.³⁶ The decrease in temperature is attributed to the developed low temperature crosslinker used, which opens to the highly reactive *o*-quinodimethane intermediate at 150 °C, which then react with each other to form

the stable benzocyclooctadiene entities, thus crosslinking the linear polymer precursor into an aqueous soluble three-dimensional architecture. The resulting chain collapsed nanoparticle was characterized through routine GPC techniques which displayed a shift in retention time in comparison to the linear precursor along with a lower molecular weight which is a clear indication of change in conformation of polymer precursor and the significant improvement of the polydispersity. (Figure 1, Table 1).

Dynamic light scattering (DLS) substantiated this observation, illustrating a size of 35 ± 2 nm for the collapsed nanoparticles. This data correlates with SEC and NMR measurements and supports a successful nanoparticle formation. Moreover, UV-Vis and fluorescence microscopy displayed absorption and emission peaks at 370 and 438 nm, respectively, with a quantum efficiency of 5.1%. These results are in agreement when compared to the linear polymer precursor emission wavelengths, with an increase in the consequential PL intensity (Figure 2). With an increase in the quantum efficiency of the nanoparticle to the linear precursor, there is an obvious site-isolation effect, which is anticipated from the intramolecular chain collapse process.

Due to the excellent aqueous solubility of the nanoparticle system, it would be advantageous to expand the applicability through the introduction of functionalities to the macromolecule, which would enhance the applicability of this structure.

The presence of acrylic acids allow the formation of amide bonds by reacting amine terminated units, adding to the versatility of the desired molecule. With ~3000 available carboxylic acid units, determined from NMR, we targeted to pegylate around 30–40% groups via the attachment of amine terminated poly(ethylene glycol) (PEG) units. PEG chains were grafted to the nanoparticle through an activated chloroformate reaction utilizing *N*-methylmorpholine and isobutyl chloroformate in DMF at 0 °C.²⁸ Removal of unreacted PEG chains through dialysis against methanol in 25,000 MWCO tubing afforded the ability to further modify the nanoparticle through the attachment of a novel metal complexing unit such as the catechol functionality. As previously reported, we synthesized an amine terminated acetonide protected catechol²⁸ which is easily grafted onto the macromolecule through the same chloroformate reaction discussed above, also here we targeted for a 30% modification of the carboxylic acids. Additionally, the introduction of 200 commercially available 3-butenylamine units led the desired functionalized macromolecule (Scheme 2). Removal of the acetonide protecting groups of the functionalized water soluble semiconducting nanoparticle was possible with HCl in water followed by chelation of gadolinium by introducing $GdCl_3$ in water to the nanoparticle, yielded the final macromolecular architecture. After purification by dialysis, relaxation measurements were taken in water to determine the efficiency of the nanoparticle as a novel MRI contrast agent. The functionalized nanoparticle displayed an ionic relaxivity value of $\sim 10 \text{ mM}^{-1}\text{s}^{-1}$ (Figure 3S, supplemental). This value is notably larger than values reported for current contrast agents Omniscan[®] and Magnevist[®], displaying relaxivities of $4.2 \text{ Mm}^{-1}\text{s}^{-1}$ and $4.3 \text{ Mm}^{-1}\text{s}^{-1}$, respectively. It is evident from these results, that the functionalized water soluble semiconducting nanoparticle is able to encapsulate more paramagnetic compound than small molecules and result in an increase in the ionic relaxivity value. The data presented certainly verifies our suggestion that macromolecular architectures with larger amounts of gadolinium than small molecules inevitably lead to larger relaxivity values and accordingly a brighter contrast on an MRI scan. These results additionally indicate that the closed architecture of the collapsed nanoparticle does not produce relaxivity values as large as in reported star polymer architectures,²⁸ but imposes advantages regarding its globular design. In preliminary studies we have not seen evidence of an accumulation in specific organs or tissues. With the added allyl groups units that enhance cell uptake or targeting, the fluorescent nanoparticle can actively interact with biological species.

Conclusion

In summary, we report the synthesis of functionalized water soluble semiconducting nanoparticles through an intramolecular chain collapse technique, which show potential for fluorescence applications and imaging such as MRI. A semiconducting telechelic macroinitiator which included EO functionalized fluorene units to improve solubility was developed to polymerize t-butyl acrylates and low temperature benzocyclobutene crosslinking units to form linear ABA block copolymer precursors which allow the preparation of semiconducting nanoparticles with reasonably well-controlled size distributions. Fluorescence quantum yields as high as 5.1% have been determined for the resulting materials. The results reported here are highly encouraging with demonstrated optical properties displaying the much anticipated site-isolation effect in the formation of a three-dimensional architecture from a linear structure. These materials were functionalized through the introduction of PEG units for additional solubility and metal complexing units. Deprotection and chelation of Gd^{3+} to the nanoparticle afforded high relaxivity values of $\sim 10 \text{ mM}^{-1}\text{s}^{-1}$. Furthermore, the presence of free allyl functionalities makes the resultant material ideal for cancer cell imaging and treatment (early detection) through the introduction of cell targeted peptides as well as cell penetrating molecular transporters units.

Supplementary Material

Refer to Web version on PubMed Central for supplementary material.

Acknowledgments

Funding Sources

E.H gratefully acknowledges the National Science Foundation (NSF) for supporting this work under award CHE-0645737. C.T.A. thanks the Vanderbilt Institute of Chemical Biology for a Chemistry-Biology Interface Program Fellowship under the NIH Training GrantNo. T32 GMO65086-5.

ABBREVIATIONS

NMR	Nuclear Magnetic Resonance Spectroscopy
MRI	Magnetic Resonance Imaging
GPC	Gel Permeating Chromatography

REFERENCES

1. Bruchez M, Moronne M, Gin P, Weiss S, Alivisatos AP. *Science*. 1998; 281:2013. [PubMed: 9748157]
2. Ha TJ, Ting AY, Liang J, Caldwell WB, Deniz AA, Chemla DS, Schultz PG, Weiss S. *Proc. Natl. Acad. Sci.* 1999; 96:893. [PubMed: 9927664]
3. Yildiz A, Forkey JN, McKinney SA, Ha T, Goldman YE, Selvin PR. *Science*. 2003; 300:2061. [PubMed: 12791999]
4. Abbondanzieri EA, Bokinsky G, Rausch JW, Zhang JX, Le Grice SFJ, Zhuang XW. *Nature*. 2008; 453:184. [PubMed: 18464735]
5. Eggeling C, Widengren J, Rigler R, Seidel CAM. *Anal. Chem.* 1998; 70:2651. [PubMed: 21644785]
6. Michalet X, Pinaud FF, Bentolila LA, Tsay JM, Doose S, Li JJ, Sundaresan G, Wu AM, Gambhir SS, Weiss S. *Science*. 2005; 307:538. [PubMed: 15681376]
7. Liu W, Howarth M, Greytak AB, Zheng Y, Nocera DG, Ting AY, Bawendi MG. *J. Am. Chem. Soc.* 2008; 130:1274. [PubMed: 18177042]

8. Yao J, Larson DR, Vishwasrao HD, Zipfel WR, Webb WW. *Proc. Natl. Acad. Sci.* 2005; 102:14284. [PubMed: 16169907]
9. Wang L, Wang KM, Santra S, Zhao XJ, Hilliard LR, Smith JE, Wu JR, Tan WH. *Anal. Chem.* 2006; 78:646.
10. Friend RH, Gymer RW, Holmes AB, Burroughes JH, Marks RN, Taliani C, Bradley DDC, Dos Santos DA, Bredas JL, Logdlund M, Salaneck WR. *Nature.* 1999; 397:121.
11. So F, Krummacher B, Mathai MK, Poplavskyy D, Choulis SA, Choong VE. *J. Appl. Phys.* 2007; 102
12. Chen LH, McBranch DW, Wang HL, Helgeson R, Wudl F, Whitten DG. *Proc. Natl. Acad. Sci.* 1999; 96:12287. [PubMed: 10535914]
13. Fan CH, Wang S, Hong JW, Bazan GC, Plaxco KW, Heeger AJ. *Proc. Natl. Acad. Sci.* 2003; 100:6297. [PubMed: 12750470]
14. Hudson SD, Jung HT, Percec V, Cho WD, Johansson G, Ungar G, Balagurusamy VSK. *Science.* 1997; 278:449.
15. Coates GW. *Chem. Rev.* 2000; 100:1223. [PubMed: 11749265]
16. Kobayashi H, Kawamoto S, Saga T, Sato N, Ishimori T, Konishi J, Ono K, Togashi K, Brechbiel MW. *Bioconjugate Chem.* 2001; 12:587.
17. Kobayashi H, Kawamoto S, Jo SK, Bryant HL, Brechbiel MW, Star RA. *Bioconjugate Chem.* 2003; 14:388.
18. Langereis S, de Lussanet QG, van Genderen MHP, Backes WH, Meijer EW. *Macromolecules.* 2004; 37:3084.
19. Rebizak R, Schaefer M, Dellacherie E. *Bioconjugate Chem.* 1997; 8:605.
20. Corot C, Schaefer M, Beaute S, Bourrinet P, Zehaf S, Benize V, Sabatou M, Meyer D. *Acta Radiol.* 1997; 38:91.
21. Helbich TH, Roberts TPL, Gossmann A, Wendland MF, Shames DM, Adachi M, Yang S, Huber S, Daldrup H, Brasch RC. *Magn. Reson. Med.* 2000; 44:915. [PubMed: 11108629]
22. Lebduskova P, Kotek J, Hermann P, Elst LV, Muller RN, Lukes I, Peters JA. *Bioconjugate Chem.* 2004; 15:881.
23. Mohs AM, Wang XH, Goodrich KC, Zong YD, Parker DL, Lu ZR. *Bioconjugate Chem.* 2004; 15:1424.
24. Bogdanov A, Wright SC, Marecos EM, Bogdanova A, Martin C, Petherick P, Weissleder R. *J. Drug Targeting.* 1997; 4:321.
25. Kobayashi H, Sato N, Saga T, Nakamoto Y, Ishimori T, Toyama S, Togashi K, Konishi J, Brechbiel MW. *Eur. J Nucl. Med.* 2000; 27:1334. [PubMed: 11007515]
26. Konda SD, Aref M, Wang S, Brechbiel M, Wiener EC. *Magn. Reson. Mater. Phy.* 2001; 12:104.
27. Li Y, Beija M, Laurent S, vander Elst L, Muller RN, Duong HTT, Lowe AB, Davis TP, Boyer C. *Macromolecules.* 2012; 45:4196.
28. Adkins CT, Dobish JN, Brown CS, Mayrsohn B, Hamilton SK, Udoji F, Radford K, Yankeeelov TE, Gore JC, Harth E. *Polym. Chem.* 2012; 3:390.
29. Beija M, Li Y, Duong HT, Laurent S, Vander Elst L, Muller RN, Lowe AB, Davis TP, Boyer C. *J. Mater. Chem.* 2012; 22:21382.
30. Lokling KE, Fossheim SL, Klaveness J, Skurtveit R. *J. Controlled Release.* 2004; 98:87.
31. Mikawa M, Miwa N, Brautigam M, Akaike T, Maruyama A. *J. Biomed. Mater. Res.* 2000; 49:390. [PubMed: 10602072]
32. Louie AY, Huber MM, Ahrens ET, Rothbacher U, Moats R, Jacobs RE, Fraser SE, Meade TJ. *Nat. Biotechnol.* 2000; 18:321. [PubMed: 10700150]
33. Adkins CT, Muchalski H, Harth E. *Macromolecules.* 2009; 42:5786.
34. Wu CF, Szymanski C, Cain Z, McNeill J. *J. Am. Chem. Soc.* 2007; 129:12904. [PubMed: 17918941]
35. Dobish JN, Hamilton SK, Harth E. *Polym. Chem.* 2012; 3:857.
36. Croce TA, Hamilton SK, Chen ML, Muchalski H, Harth E. *Macromolecules.* 2007; 40:6028.

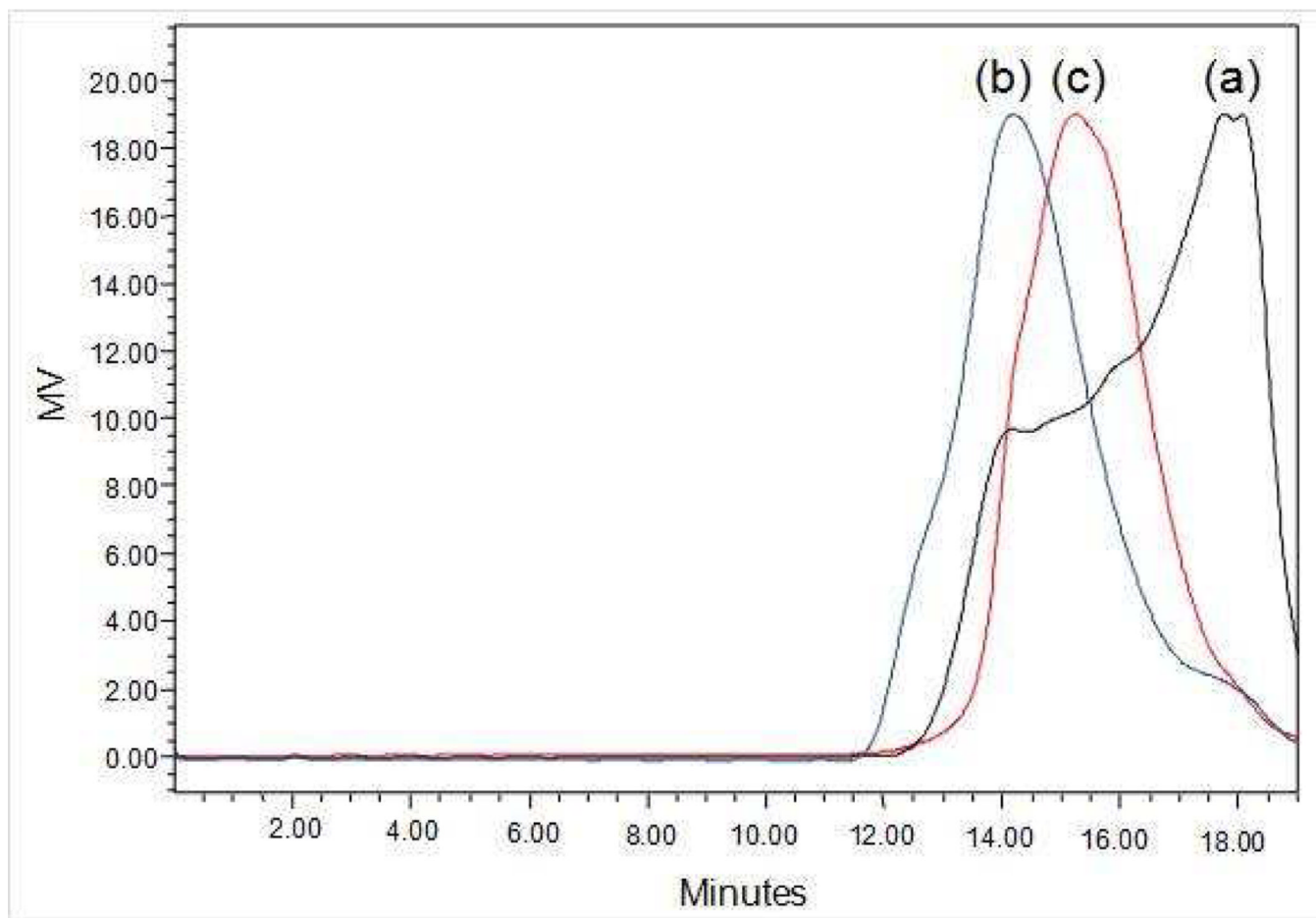


Figure 1. Comparison of gel permeation chromatography (GPC) traces for (a) EO fluorene macroinitiator, **1**, ($M_w=13,000$ Da, PDI = 4.79); (b) EO fluorene linear precursor, **4**, ($M_w = 67,000$ Da, PDI = 4.31); and (c) fluorene nanoparticle, **5**, ($M_w = 23,000$ Da, PDI = 2.87)

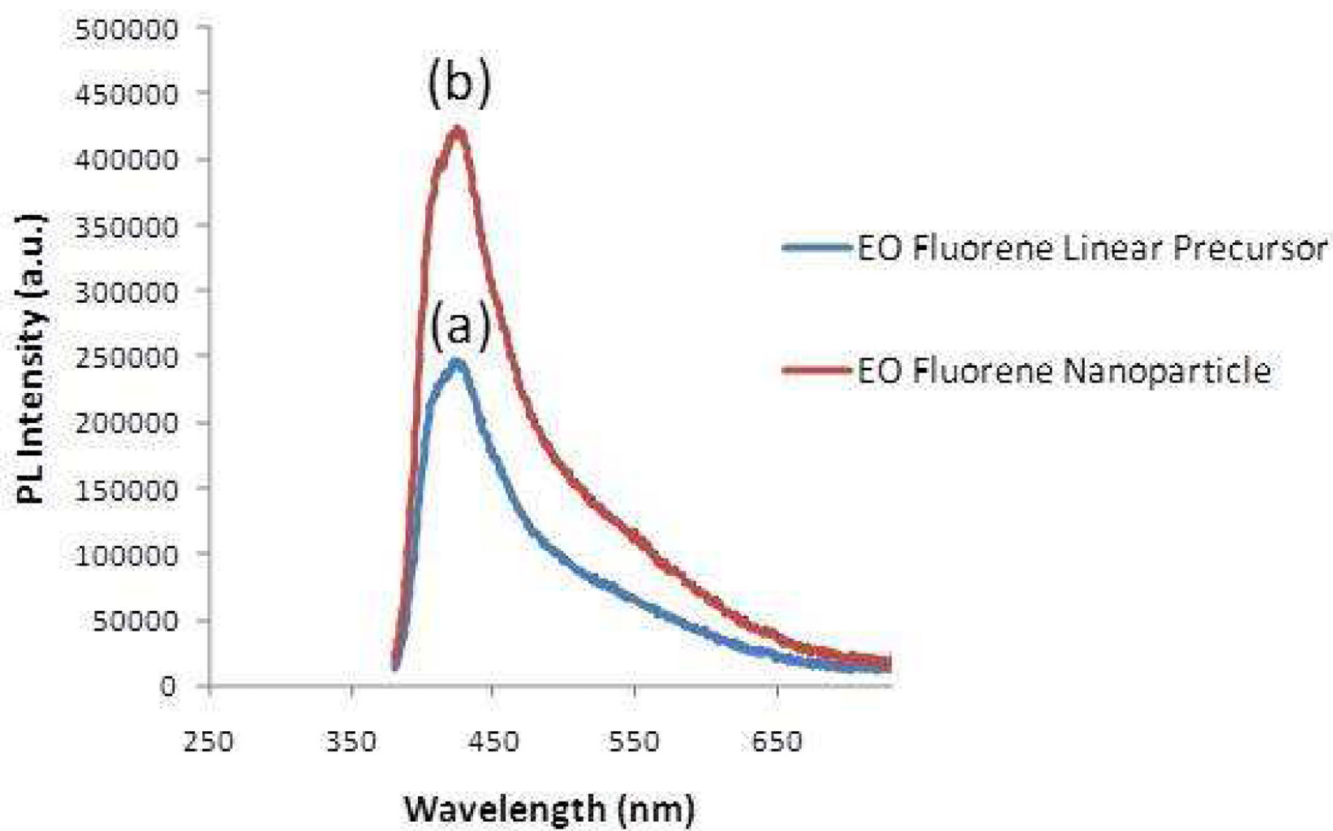
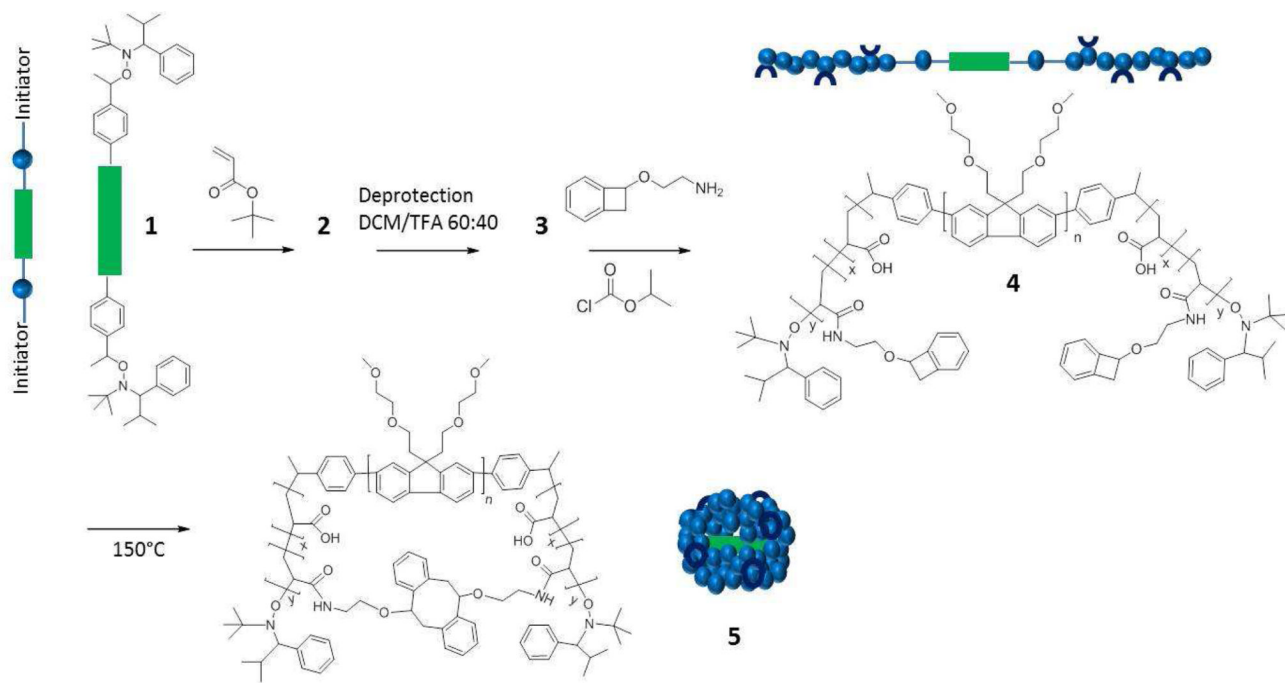
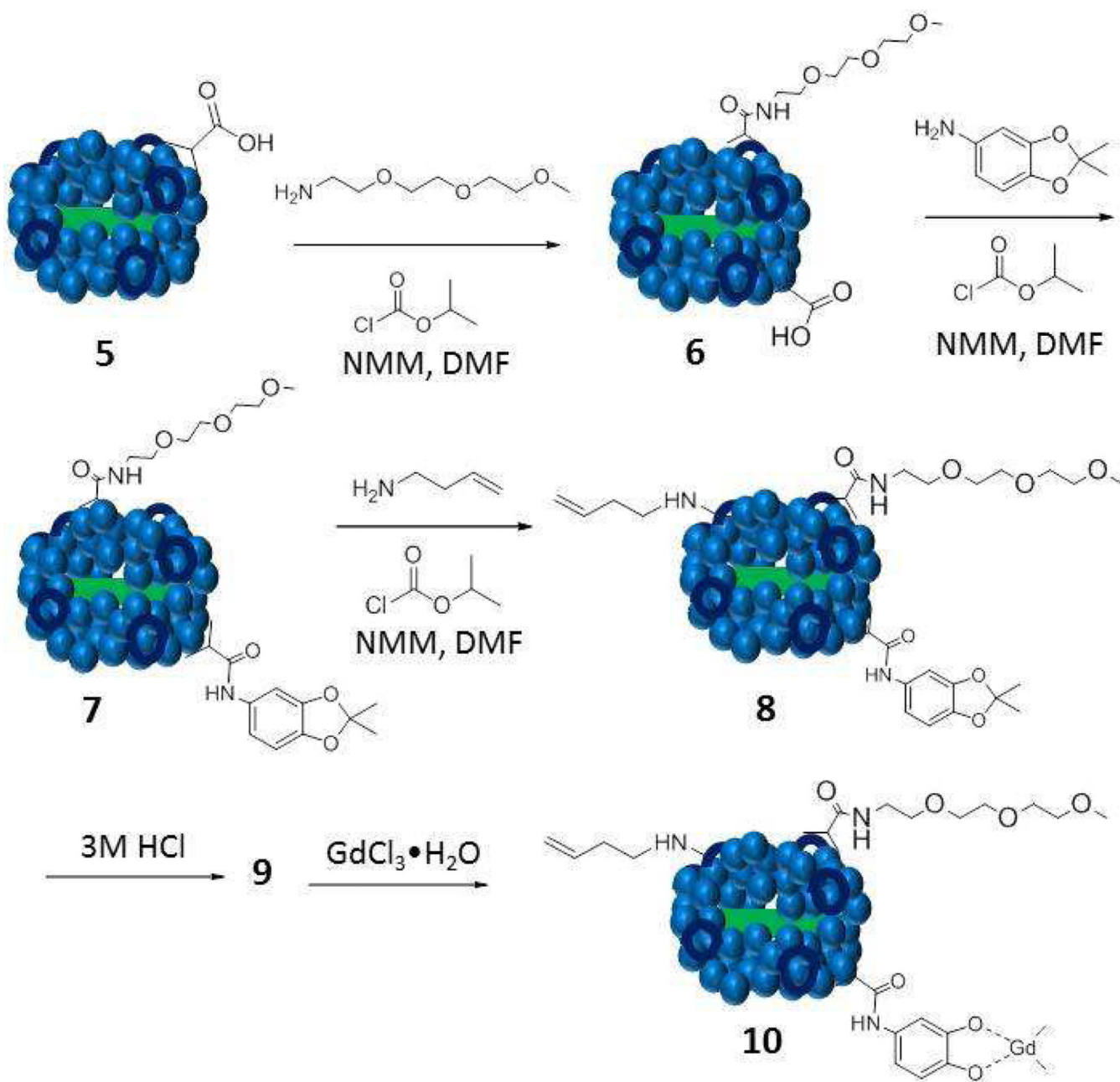


Figure 2. Photoluminescence (PL) measurements of (a) EO fluorene linear precursor **4** and (b) EO fluorene nanoparticle **5** (4×10^{-3} M in methanol).





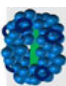
Scheme 1.
Synthesis of ethylene oxide (EO) nanoparticle



Scheme 2. Post-modification of water-soluble nanoparticle with PEG, complexing units and functional groups for thiolene-click reactions.

Characterization data for ethylene oxide (EO) fluorene macroinitiator, EO fluorene linear precursor, and EO fluorene nanoparticles.

Table 1

Symbol	Compound number	Molecular Weight Ratio	$M_{n,NMR}$ (g/mol)	M_w, RI (g/mol) ^a	PDI ^b
	1	-	19000	13000	4.79
	4	2:1:2	96000	67000	4.31
	5	-	-	23000	2.87

^a weight-average molecular weight (M_w) after purification; gel permeation chromatography (GPC) data relative to Polystyrene standards (PS) and

^b polydispersity ($PDI = M_w/M_n$), measured by gel permeation chromatography with tetrahydrofuran as eluent and integrated RI detector; Calibration with linear PS as standard.